

In Vitro Anticancer Activity of Nanoformulated Mono- and Di-nuclear Pt Compounds

Pan Wang,^[a] Jian-Wei Wang,^[b] Wen-Hua Zhang,^{*,[a]} Hongzhen Bai,^{*,[b]} Guping Tang,^[b] and David J. Young^[c]

Dedicated to Prof. Tzi Sum Andy Hor on the occasion of his 65th birthday.

Abstract: Nanoformulations of mononuclear Pt complexes *cis*-PtCl₂(PPh₃)₂ (1), [Pt(PPh₃)₂(L-Cys)]·H₂O (3, L-Cys = L-cysteinate), *trans*-PtCl₂(PPh₂PhNMe₂)₂ (4; PPh₂PhNMe₂ = 4-(dimethylamine)triphenylphosphine), *trans*-PtI₂(PPh₂PhNMe₂)₂ (5) and dinuclear Pt cluster Pt₂(μ-S)₂(PPh₃)₄ (2) have comparable cytotoxicity to cisplatin against murine melanoma cell line B16F10. Masking of these discrete molecular entities within

the hydrophobic core of Pluronic® F-127 significantly boosted their solubility and stability, ensuring efficient cellular uptake, giving in vitro IC₅₀ values in the range of 0.87–11.23 μM. These results highlight the potential therapeutic value of Pt complexes featuring stable Pt–P bonds in nanocomposite formulations with biocompatible amphiphilic polymers.

Introduction

Since the seminal discovery that cisplatin exhibited anti-proliferative behavior against *Escherichia coli* in 1965,^[1] and its approval by the US Food and Drug Administration (FDA) in 1978 for the treatment of metastatic testicular, ovarian, and bladder cancers, cisplatin and related Pt-based complexes have been a mainstay of chemotherapeutic antitumor regimens.^[2] Other FDA or regionally approved Pt-based drugs include carboplatin, oxaliplatin, nedaplatin, heptaplatin, and lobaplatin.^[3] In addition to these clinically approved chemotherapeutic drugs, a huge number of Pt-based coordination complexes supported by diverse ligand types have proven effective in cellular and animal cancer models.^[2,4]

Small molecular drugs, including Pt-based drugs, have been widely integrated with nanotechnology to improve their therapeutic efficacy.^[5] One successful example is the liposomal formation (e.g. SPI-77,^[6] Lipoplatin,^[7] LiPlaCis^[8]) of cisplatin within nano-sized hydrophilic bilayers of phospholipids.^[8a,9] Liposomal encapsulation enhances the circulation time of the drug, leading to increased drug accumulation at the tumor site

through the enhanced permeability and retention (EPR) effect with a simultaneous reduction of adverse side effects.^[7a,8a,9]

In addition to the EPR effect (passive targeting),^[10] nanotechnology allows for multiple therapeutic modalities to be integrated into one formulation. These combinative therapies^[11] can achieve targeting capability^[12] and may combine with gene therapy, radiotherapy, photodynamic therapy and/or immunotherapy.^[3,5e,11c,13] In this work, we have studied the nanoparticle formation of a class of mononuclear and dinuclear Pt-based complexes featuring P- and/or S-based ligands using amphiphilic polymer Pluronic® F-127.^[14] These complexes included mononuclear *cis*-PtCl₂(PPh₃)₂ (1),^[15] [Pt(PPh₃)₂(L-Cys)]·H₂O (3, L-Cys = L-cysteinate), *trans*-PtCl₂(PPh₂PhNMe₂)₂ (4, PPh₂PhNMe₂ = 4-(dimethylamine)triphenylphosphine)^[16] and *trans*-PtI₂(PPh₂PhNMe₂)₂ (5), as well as a dinuclear Pt cluster Pt₂(μ-S)₂(PPh₃)₄ (2).^[17] We hypothesized that the use of a strong-field P-based ligand would facilitate the dissociation of Pt–Cl (1), Pt–S (2, 3), or Pt–N (3) bonds at the *trans* position to facilitate DNA cross-linking, similar to the action mechanism of cisplatin.

Glutathione (GSH), an S-based reducing species over-expressed in cancer cells, exhibits similar donor strength to Cl, S, and N, and may also serve to accelerate dissociation of Pt–Cl (1), Pt–S (2, 3) and Pt–N (3) bonds to enhance DNA binding. We herein report the synthesis and structural relationships of 1–5, their nanoparticle formulation using Pluronic® F-127 and anti-cancer properties against murine melanoma B16F10 cells line. The favorable results obtained with these nanocomposites indicate that formulations of Pt complexes bearing stable Pt–P bond may be promising leads for new anticancer chemotherapies.

Results and Discussion

There is still an intense research interest in developing novel Pt-based therapeutics for cancer treatment four decades after the

[a] P. Wang, Prof. W.-H. Zhang
College of Chemistry, Chemical Engineering and Materials Science
Soochow University
Suzhou 215123 (P. R. China)
E-mail: whzhang@suda.edu.cn

[b] Dr. J.-W. Wang, Dr. H. Bai, Prof. G. Tang
Department of Chemistry
Zhejiang University
Hangzhou 310028 (P. R. China)
E-mail: hongzhen_bai@zju.edu.cn

[c] Prof. D. J. Young
College of Engineering Information Technology & Environment
Charles Darwin University
Darwin, Northern Territory 0909 (Australia)

Supporting information for this article is available on the WWW under <https://doi.org/10.1002/asia.202100901>

This manuscript is part of a special collection on Metals in Functional Materials and Catalysis.

approval of cisplatin.^[4c,5a,9] A primary challenge is to improve patient benefit by reducing damage to normal tissues resulting in nausea and hair loss among other side effects. This can potentially be achieved through nanotechnology to provide stable and biocompatible particles of suitable size (e.g. in the range of 50–200 nm) for targeted drug delivery.^[18] Multiple therapeutic and/or diagnostic modalities have been integrated to try and achieve synergistic and spatiotemporal treatment.^[19] Aside from nanomaterial assembly, carefully designed Pt-based complexes can also be used to achieve fine-tuning of the drug-biomolecule interaction.^[4c,e,f,20]

A central Pt(II/IV) coordinated by specific ligand types can achieve nucleic acid selectivity and apoptosis.^[4b,21] A well-known example is oxaliplatin that can induce immunogenic cell death (ICD) in the treatment of colon cancer, while cisplatin and other clinically adapted platinum drugs fail to do so.^[4e,22] ICD is a critical step in immunotherapy by priming T-cell activation. Its combination with immunotherapeutic modalities, such as PD-1/PD-L1 therapy is expected to show clinical potential for the treatment of tumors that are resistant to immunotherapy alone (cold tumor).^[23] Ang *et al.*^[4e,24] screened a series of Pt-complexes and found that those bearing a biscarbene ligand, which they termed 'PlatinER' exhibit superior ICD properties.

It is well-established that the major mechanism of cisplatin chemotherapy is that the complex becomes activated intracellularly by the aquation of one of the two Cl⁻ 'leaving' groups, and subsequently binds to DNA, forming metallated DNA adducts.^[2,25] The driving force is the superior donor strength of NH₃ relative to Cl⁻ and thus the Pt–Cl bond *trans* to Pt–NH₃ is more susceptible to H₂O exchange. By analogy, we speculate that for Pt-based species with phosphine ligands, such as *cis*-PtCl₂(PPh₃)₂ (**1**, Scheme 1), the two Pt–Cl bonds that are *trans* to the two Pt–P bonds should labile, facilitating DNA cross-linking, leading to cell apoptosis. The lower Cl⁻ concentration of 10–20 mM in the cytoplasm relative to blood (0.1 M) also contributes to Pt–Cl bond dissociation.^[26]

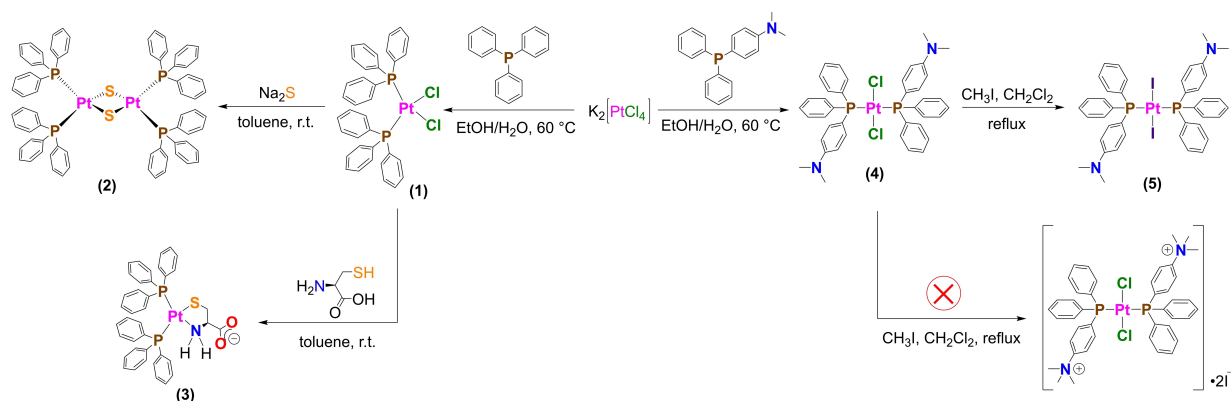
Syntheses and structural characterization of 1–5

Mononuclear **1** and dinuclear cluster **2** were readily synthesized from the reaction of K₂PtCl₄ and PPh₃ following reported protocols (Scheme 1).^[27] The facile inclusion of the S atom into the coordination sphere of **1** to give dinuclear cluster **2** prompted us to study its reaction with S-based amino acids contain SH, as the transactivator of transcription (TAT) peptide and internalizing arginine-glycine-aspartic acid (iRGD) cyclic peptide have demonstrated transmembrane and/or tumor-targeting, in addition to other useful properties.^[28] The reaction of **1** and L–Cys in toluene at room temperature gave rise to zwitterionic **3** in 40% yield. The positive charges of Pt²⁺ in **3** are balanced by the deprotonated SH and one deprotonated and uncoordinated carboxylate.

The hyperpolarized membrane potential of mitochondria in cancer cells has been exploited in anticancer drug design by, for example, incorporating cationic functionality.^[4c,29] In this regard, the use of ligand PPh₂PhNMe₂ is preferred as the –NMe₂ function in the ligand is assumed to readily react with MeI to give the –[NMe₃]⁺ cation.^[30] The reaction of K₂PtCl₄ and PPh₂PhNMe₂ gave rise to **4** (33% yield) wherein a pair of PPh₂PhNMe₂ ligands and a pair of Cl is in an unexpected *trans* configuration (Scheme 1).^[27]

Notably, the reaction of **4** with a large excess of MeI in CH₂Cl₂ failed to produce the cationic compound as expected (Scheme 1), but gave mononuclear complex **5** wherein the two Cl⁻ of **4** were replaced by I⁻ (63% yield) with the retention of the *trans* configuration. It is notable that **5** was insoluble in most solvents such as DMSO, DMF, MeCN, and CHCl₃, and only slightly soluble in CH₂Cl₂ and MeOH. The strong propensity of Pt²⁺ toward soft I⁻ coupled with the low solubility of **5** might be the reason for the unsuccessful formation of the cationic species.

Complexes **1–4** were characterized by ¹H, ¹³C, and ³¹P NMR spectroscopy in CDCl₃ (Figures S1–S4; **5** was too insoluble). Single proton decoupled ³¹P resonances at 14.3 ppm (**1**, Figure S1c), 28.0 ppm (**2**, Figure S2c), 10.7/18.4 ppm (**3**, doublet, Figure S3c), and 18.3 ppm (**4**, Figure S4c) indicated high purity. It should be noted that when the single crystals of **4** were immersed in CD₂Cl₂ overnight, its ³¹P NMR indicated that the



Scheme 1. Synthesis of 1–5 using K₂[PtCl₄] as the starting material.

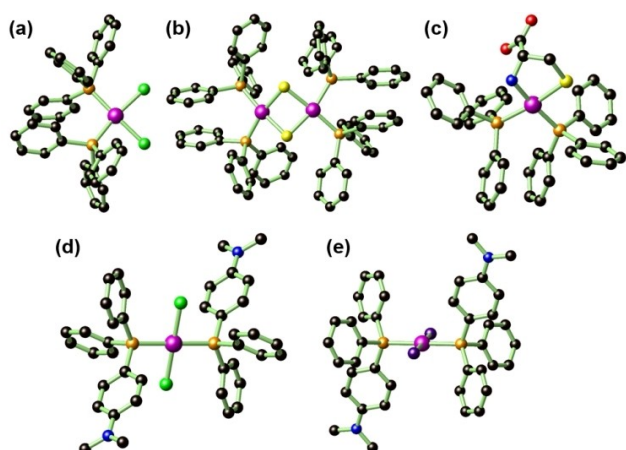


Figure 1. Single crystal structure of 1 (a), 2 (b), 3 (c), 4 (d), and 5 (e). Colour codes: Pt (dark magenta), P (orange), S (yellow), Cl (green), I (purple), O (red), N (blue), C (black). All hydrogen atoms and solvates are omitted for clarity.

singlet at 18.6 ppm shifted to 12.0 ppm, suggesting a *trans-to-cis* structural change (Figure S5a, and S5b). Similar observation was also made by Brune *et al.*^[16] who demonstrated that 4 undergoes a *trans-to-cis* structural change in CH₂Cl₂ at r.t. The purities of all five complexes were confirmed by microanalyses and Fourier-transform infrared (FT-IR) spectra. Solid-state structures were elucidated by single-crystal X-ray diffraction (Table 1, Figure 1).

The *cis* configuration of 1 (Figure 1a) and the dimeric structure of 2 (Figure 1b) have been reported previously.^[15,31] Both the S and N atoms in the L–Cys ligand of 3 coordinate to the Pt²⁺ (Figure 1c) to give a stable five-membered metallo-

cycle. The two C–O bond distances of the carboxylate have nearly identical values (C3–O1 = 1.251(13) Å; C3–O2 = 1.241(13) Å), an indication of a conjugated, deprotonated, and uncoordinated carboxylate, and thus consistent with the zwitterionic nature of 3.^[32]

The synthesis of 5 (Figure 1e) from 4 (Figure 1d) was confirmed by their distinctive Pt–Cl (2.3074(14) Å; 4) and Pt–I (2.6177(4) Å; 5) distances. The X–Pt–X bonds (X=Cl and I) exhibited torsional freedom concerning the P–Pt–P axis. The C–P–Pt–Cl and C–P–Pt–I torsional angles were –133.8° (4) and 104.7° (5), respectively.

Nanoparticle self-assembly of 1–4 using Pluronic® F-127

One of the key obstacles when using Pt-based drugs, including cisplatin, for chemotherapy is their limited solubility. As a consequence, Pt drugs generally exhibit short circulation times with low accumulation at the tumour site, leading to side effects. Cisplatin, for example, has notable nephron- and ototoxicity.^[33] Nano-carriers based on the self-assembly of amphiphilic small molecules or block copolymers, such as DSPE-PEG2K^[34] and PEO-PPO-PEO (Pluronic polymer micelles)^[14,35] have been widely used to improve the solubility of Pt drugs. When assembled in aqueous solution with these (usually lipophilic) drugs, the hydrophobic segment of the amphiphilic molecules aggregates to form the core of the micelle, functioning as the host region to encapsulate the drug, while the hydrophilic end exposed to water endows water solubility, stability, and biocompatibility.

We employed Pluronic® F-127 (PEO₉₉-PPO₆₇-PEO₉₉) as the host material to prepare nanoparticles of 1–4 (the nanoparticle

Table 1. Summary of crystallographic data for 1–5.

| Compounds | 1 | 2 | 3 | 4 | 5 |
|---|---|---|--|--|---|
| Formula | C ₃₆ H ₃₀ Cl ₂ P ₂ Pt | C ₇₂ H ₆₀ P ₄ Pt ₂ S ₂ | C ₃₉ H ₃₇ NO ₃ P ₂ PtS | C ₄₀ H ₄₀ Cl ₂ N ₂ P ₂ Pt | C ₄₀ H ₄₀ I ₂ N ₂ P ₂ Pt |
| FW | 790.52 | 1503.38 | 856.78 | 876.67 | 1059.57 |
| Crystal system | monoclinic | Triclinic | Orthorhombic | Triclinic | Triclinic |
| Space group | <i>P</i> 2 ₁ / <i>c</i> | <i>P</i> -1 | <i>P</i> 2 ₁ 2 ₁ | <i>P</i> -1 | <i>P</i> -1 |
| <i>a</i> (Å) | 32.373(2) | 12.1221(7) | 10.430(3) | 9.9846(9) | 8.4088(4) |
| <i>b</i> (Å) | 9.5967(6) | 13.2267(8) | 16.109(4) | 10.0248(9) | 10.5983(5) |
| <i>c</i> (Å) | 19.4538(12) | 21.1703(12) | 20.459(5) | 10.4448(10) | 11.1794(6) |
| α (°) | 90.00 | 83.9490(17) | 90.00 | 86.043(3) | 99.188(2) |
| β (°) | 94.520(2) | 77.3162(17) | 90.00 | 68.439(3) | 97.398(2) |
| γ (°) | 90.00 | 77.3162(17) | 90.00 | 65.086(3) | 104.277(2) |
| <i>V</i> (Å ³) | 6025.0(6) | 3293.1(3) | 3437.6(15) | 877.25(14) | 938.30(8) |
| <i>Z</i> | 8 | 2 | 4 | 1 | 1 |
| ρ_{calc} g cm ⁻³ | 1.743 | 1.516 | 1.655 | 1.659 | 1.875 |
| μ , mm ⁻¹ | 8.029 | 4.444 | 4.275 | 4.275 | 5.500 |
| <i>F</i> (000) | 3104 | 1480 | 1704 | 436 | 508 |
| Total reflns. | 153469 | 190861 | 117966 | 92195 | 20171 |
| Uniq. reflns. | 13291 | 16370 | 8555 | 3868 | 3300 |
| Reflns. (<i>I</i> ≥ 2 σ (<i>I</i>)) | 12222 | 9750 | 6514 | 3681 | 2675 |
| <i>R</i> _{int} | 0.0517 | 0.2123 | 0.2332 | 0.1014 | 0.1101 |
| Parameters | 739 | 721 | 425 | 214 | 216 |
| <i>R</i> ₁ ^[a] | 0.0274 | 0.0500 | 0.0485 | 0.0396 | 0.0343 |
| <i>wR</i> ₂ ^[b] | 0.0707 | 0.0851 | 0.0917 | 0.0885 | 0.0527 |
| <i>GOF</i> ^[c] | 1.079 | 1.013 | 1.008 | 1.098 | 1.062 |
| $\rho_{\text{max}}/\rho_{\text{min}}$ e Å ⁻³ | 0.831/–2.356 | 0.904/–1.290 | 2.690/–2.377 | 2.235/–1.775 | 1.359/–1.365 |

[a] $R_1 = \sum ||F_o| - |F_c|| / \sum |F_o|$, [b] $wR_2 = \{\sum [\omega(F_o^2 - F_c^2)^2] / \sum [\omega(F_o^2)]\}^{1/2}$, and [c] $GOF = \{\sum [\omega(F_o^2 - F_c^2)^2] / (n-p)\}^{1/2}$, where *n* is the number of reflections, and *p* the total number of parameters refined.

of 5 could not be prepared due to its low solubility).^[14] Stirring a DMSO or CH₂Cl₂ solution containing Pt complex and Pluronic® F-127 with excess water gave a homogenous solution. Dialysis (molecular weight cut-off: 3500) and lyophilization gave the target materials.

Transmission electron microscopy (TEM, Figure 2) showed that 1–4 formed regular, spherical particles with Pluronic® F-127, of ca 300 nm (1), 300 nm (2), 80 nm (3), and 500 nm (4) in diameter. The size of these particles was suitable for *in vitro* cytotoxicity analysis. The zeta potential of the nanoparticles of 1 (0.13 mV, Figure S6a), 2 (12.5 mV, Figure S6b), 3 (−3.79 mV, Figure S6c), and 4 (6.47 mV, Figure S6d) was close to zero which is conducive for long circulation times to elicit the EPR effect.

The ³¹P NMR of these nanoparticles in CDCl₃ show that there is no obvious chemical shift for those of 1 (Figure S7a) and 3 (Figure S7c), indication of structural retention upon particle formation. However, for that of 2 (Figure S7b), the singlet at 28.0 ppm disappeared, accompanied by the generation of two new peaks at 21.4 ppm and 14.3 ppm. This is likely due to decomposition of the complex (e.g. by Pt–S bond breaking). Furthermore, for that of 4 (Figure S7d), the singlet at 18.3 ppm also shifted to 12.3 ppm, this resembles that for the single crystal of 4 in CD₂Cl₂ and indicating a *trans-to-cis* conversion during the particle preparation.

Cytotoxicity evaluation by MTT assay

Murine melanoma B16F10 was used as the model cell line to evaluate the anti-proliferation potential of the nanoformulations of 1–4 using the MTT assay (MTT = 3-[4,5-dimethylthiazol-2-yl]-2,5 diphenyl tetrazolium bromide). B16F10 cells were first cultured in Dulbecco's Modified Eagle Medium (DMEM) contain-

ing 10% fetal bovine serum (FBS) and 1% penicillin/streptomycin (P/S), and then transferred to a 96-well cell culture plate (1 × 10⁴ cells per well) in DMEM (10% FBS and 1% PS) and cultured for 16 h for attachment. The culture medium was then removed, followed by the addition of the nanoformulations of 1–4 in DMEM (with free DMEM as the control, *n* = 5) for an additional 20 h. MTT (0.5 mg mL^{−1}) in DMEM was then added to replace the cell culture medium, this was followed by replacement of the medium by DMSO to dissolved the formazan crystals formed for spectrophotometric measurement at 570 nm.

Nanoformulations of 1–4 exhibited obvious cytotoxicity (20 h) against melanoma cells (Figure 3) with IC₅₀ of 5.32 μM (1, Figures 3a and 3b), 0.87 μM (2, Figures 3c and 3d), 11.23 μM (3, Figures 3e and 3f), and 2.82 μM (4, Figures 3g and 3h). These values are comparable to that of cisplatin (7.4 μM, 24 h),^[36] Pt-Pyrazole complexes [Pt(Pz–CH₃)₂Cl₂] (8.3 μM, 72 h),^[37] [Pt(Pz–F)₂Cl₂] (17.7 μM, 72 h),^[37] Pt–Cu heterometallic cluster [CuCl(isad)Pt(NH₃)Cl₂] (0.63 μM, 24 h),^[38] β-cyclodextrin encapsulated *trans*-dichloro-(dipyridine)platinum(II) (0.71 μM, 20 h),^[39] and cisplatin human serum albumin nanoparticles (150 μM, 24 h).^[40]

It is interesting to note that dinuclear cluster 2 exhibited the lowest IC₅₀ value, indicating that the presence of S atoms in the cluster might play a non-innocent role (e.g. as a convenient leaving group). By contrast, compound 3 bearing the L–Cys ligand exhibited the highest IC₅₀ value presumably due to the tight binding of this chelating ligand. It is also notable that the mononuclear compound 4 with *trans* stereochemistry also

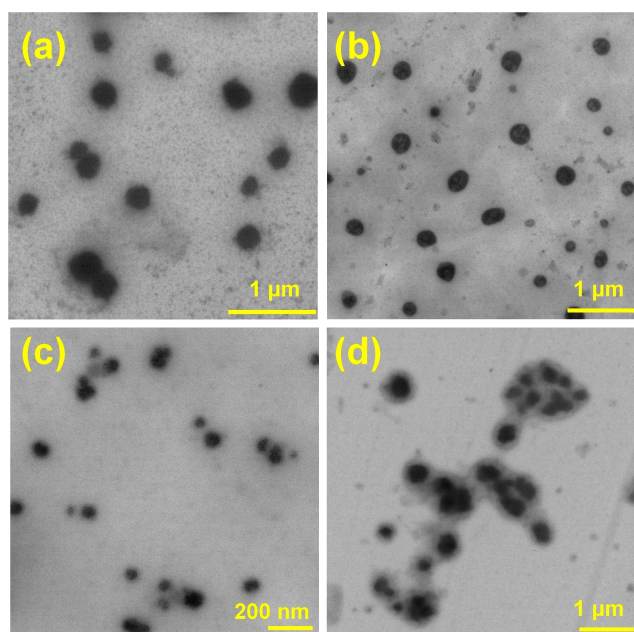


Figure 2. TEM images of 1 (a), 2 (b), 3 (c), and 4 (d) nanoparticles formed with Pluronic® F-127.

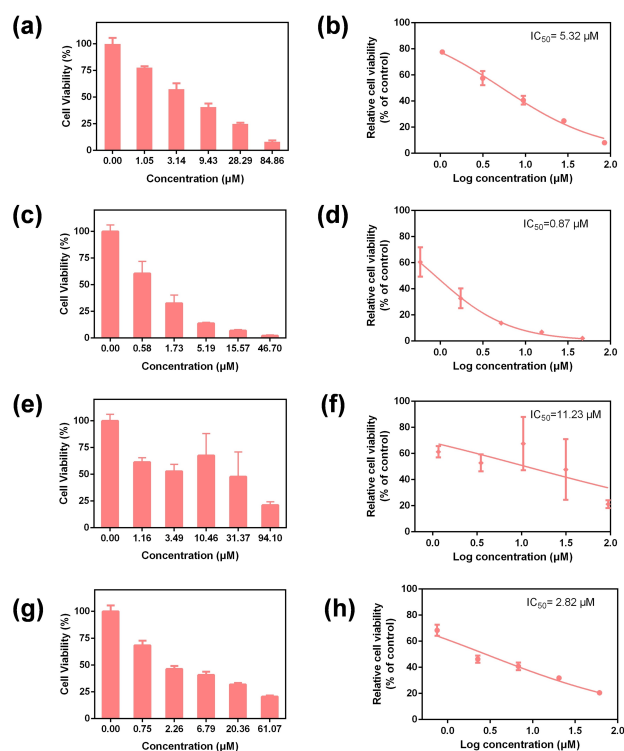


Figure 3. Cell viability and IC₅₀ (μM) results for nanoformulations of 1 (a, b), 2 (c, d), 3 (e, f), and 4 (g, h) against murine melanoma B16F10 cells (*n* = 5).

exhibited good cytotoxicity. This might be due to a facile *trans*-to-*cis* configurational change in solution or within the cells.^[41]

Conclusion

We have reported the synthesis of a class of Pt-based nano-formulations as potential cancer chemotherapies. We observed that the use of strong-field ligands such as non-toxic PPh₃ made for easier material preparation to yield stable products. Given a large number of P-based ligands, such as the monotopic PPh₃ and chelating phosphines, many Pt–P complexes can be expected with the auxiliary ligands *trans* to P readily removed to influence the cytotoxicity of the drug. In addition, the very low IC₅₀ value for **2** indicates that the presence of S atoms in the compound may be important. Moreover, diverse chemistry can be explored by taking advantage of the nucleophilicity of S, as elegantly demonstrated by Hor et al.^[17,42] It should also be noted that the *in vitro* data obtained herein is still preliminary and substantial amount work is still need in the future, such as the drug loading in the cells, DNA binding kinetic studies, the possibly subtle biological roles of S, as GSH and related biomolecules bearing S atoms are found to coordinate with Pt ions and sequester them from the cell, leading to drug resistance.^[43]

Experimental Section

General

Compounds **1** and **2** were synthesized following the reported protocols with slightly modified procedures.^[27] Potassium tetrachloroplatinate(II) (Pt > 46.5%, Laajoo), triphenylphosphine (PPh₃, > 95%, Aladdin), 4-(dimethylamino)triphenylphosphine (PPh₂PhNMe₂, 95%, Yuanye), iodomethane (MeI, 98%, Energy Chemical), Pluronic® F-127 (molecular weight: 12600, Sigma-Aldrich), Platinum standard solution (> 95%, Aladdin) and other reagents were obtained from commercial sources and used as received. The nuclear magnetic data of ¹H, ¹³C, and ³¹P NMR were obtained from the Varian UNITY plus-400/plus-600 NMR spectrometer. FT-IR spectra were measured on a Varian 1000 FT-IR spectrometer as KBr disks (400–4000 cm⁻¹). Elemental analyses for C, H, and N were performed on a Carlo-Erba CHNO–S micro-analyzer. The transmission electron microscope (TEM) images were obtained by dropping the sample in water onto the copper net under the HT7700 transmission electron microscope. The determination and analysis of Pt element content were measured on the inductively coupled plasma mass spectrometry (ICP-MS) of Varian 710-ES. Zeta potential is measured on LA-95052 laser particle size analyzer using dynamic light scattering technology (DLS).

Synthesis of *cis*-PtCl₂(PPh₃)₂ (**1**)

PPh₃ (2.50 g, 9.53 mmol) was added to anhydrous ethanol (30.0 mL) and the mixture heated to boiling. K₂PtCl₄ (2.00 g, 4.8 mmol) in 25.0 mL aqueous solution was then slowly added to immediately give white precipitate. The mixture was stirred at 60 °C for 2 hours and then filtered, washed with hot water, hot ethanol and ethyl ether to obtain the title compound. Yield: 3.58 g (94% based on Pt). Colorless crystals were grown by diffusing ether into a CH₂Cl₂

solution of **1**. Elemental analysis (%) for C₃₆H₃₀Cl₂P₂Pt: Calcd: C 54.67, H 3.79; found: C 54.63, H 3.79. IR (KBr disc, cm⁻¹): 3051(w), 1480(m), 1434(m), 1314(w), 1183(w), 1163(w), 1097(m), 1090(m), 1072(w), 999(w), 925(s), 755(vs), 744(vs), 694(vs). ¹H NMR (400 MHz, CDCl₃): δ 7.56–7.42 (m, 12H), 7.33 (t, *J* = 7.3 Hz, 6H), 7.17 (t, *J* = 7.1 Hz, 12H). ¹³C NMR (100 MHz, CDCl₃) δ 135.0 (t, *J* = 5.2 Hz), 130.9, 129.9 (t, *J* = 25.8 Hz), 128.0 (t, *J* = 5.7 Hz). ³¹P NMR (162 MHz, CDCl₃): δ 14.3.

Synthesis of Pt₂(μ-S)₂(PPh₃)₄ (**2**)

Compound **1** (0.50 g, 0.63 mmol) and Na₂S·9H₂O (0.75 g, 3.12 mmol) were stirred in toluene (70.0 mL) at r.t. for 2 days to obtain yellow-orange precipitate, which was filtered, washed with Et₂O and water, and air-dried to give the title compound. Orange-yellow single crystals were obtained by evaporating a MeOH solution of **2** at r.t. Yield 0.41 g (87% based on Pt). Elemental analysis (%) for C₇₂H₆₀P₄Pt₂S₂: Calcd: C 57.52, H 4.02; found: C 55.77, 3.98. IR (KBr disc, cm⁻¹): 3047(w), 1571(w), 1477(w), 1433(m), 1311 (w), 1181(w), 1095(s), 1028(w), 997(w), 743(s), 735(s), 688(s). ¹H NMR (400 MHz, CDCl₃) δ 7.42 (d, *J* = 6.9 Hz, 24H), 7.07 (t, *J* = 7.3 Hz, 12H), 6.93 (t, *J* = 7.6 Hz, 24H). ¹³C NMR (100 MHz, CDCl₃) δ 135.1, 128.9, 126.9. ³¹P NMR (162 MHz, CDCl₃) δ 28.0.

Synthesis of [Pt(PPh₃)₂(L–Cys)]·H₂O (**3**)

Compound **1** (0.15 g, 0.19 mmol) and L–Cysteine (0.11 g, 0.95 mmol) were suspended in 10.0 mL toluene. The resulting mixture was stirred at r.t. for three days to give a light-yellow precipitate, which was isolated by centrifugation. The precipitate was dissolved in CH₂Cl₂ and centrifuged, evaporation of the CH₂Cl₂ solution provided **3** as a crude product, which was then purified by column chromatography using CH₂Cl₂/MeOH (10:1; v/v) as the eluent. Yield 64.8 mg (40% based on Pt). Elemental analysis (%) for C₃₉H₃₇NO₃P₂PtS: Calcd: C 53.52, H 4.15, N 1.60; found: C 52.42, H 4.58, N 1.56. IR (KBr disc, cm⁻¹): 3051(w), 2920(w), 2854(w), 1607(vs), 1481(s), 1435(w), 1333(s), 1186(w), 1094(s), 997 (w), 744 (s). ¹H NMR (400 MHz, CDCl₃) δ 7.46–7.27 (m, 24H), 7.21 (td, *J* = 7.8, 2.6 Hz, 6H), 4.78–4.55 (m, 1H), 3.63 (s, 2H), 3.07–2.85 (m, 2H). ¹³C NMR (100 MHz, CDCl₃) δ 172.4, 134.4 (dd, *J* = 55.2, 11.1 Hz), 131.6 (dd, *J* = 44.0, 2.2 Hz), 128.7 (dd, *J* = 106.0, 11.2 Hz), 69.0, 35.7. ³¹P NMR (162 MHz, CDCl₃) δ 18.4 (d, *J* = 21.6 Hz), 10.7 (d, *J* = 21.0 Hz) ppm.

Synthesis of *trans*-PtCl₂(PPh₂PhNMe₂)₂ (**4**)

Compound **4** was synthesized using a method similar to that described for **1**, except that PPh₂PhNMe₂ was used instead of PPh₃. PPh₂PhNMe₂ (1.47 g, 4.83 mmol) was dissolved in refluxing EtOH. K₂PtCl₄ (1.00 g, 2.41 mmol) in 12.5 mL H₂O was then slowly introduced to form a pale yellow precipitate immediately. The mixture was stirred overnight at 60 °C to give a large amount of light yellow precipitate which was filtered and washed with hot water, hot ethanol and ether, and air-dried to give the crude product. Purification was achieved by column chromatography using CH₂Cl₂/MeOH (2:1; v/v) as the eluent. Yield: 0.69 g (33% based on Pt). Pale yellow single crystals of **4** were obtained by slow evaporation of a CH₂Cl₂ and MeOH mixed solution. Elemental analysis (%) for C₄₀H₄₀Cl₂N₂P₂Pt: Calcd: C 54.80, H 4.60; found: C 54.33, H 4.60. IR (KBr disc, cm⁻¹): 3051(w), 2852(w), 1595(s), 1513(m), 1476(w), 1433(m), 1361(s), 1292(w), 1227(w), 1201(s), 1104(s), 1094 (s), 999(w), 943(w), 811(s), 740(s), 690(vs), 623(w). ¹H NMR (400 MHz, CDCl₃): δ 7.74–7.59 (m, 12H), 7.44–7.29 (m, 12H), 6.74–6.65 (m, 4H), 2.99 (s, 12H). ¹³C NMR (100 MHz, CDCl₃) δ 137.0 (t, *J* = 6.9 Hz), 135.0 (t, *J* = 5.9 Hz), 130.1, 127.8 (t, *J* = 5.3 Hz), 111.4 (t, *J* = 5.8 Hz), 40.1. ³¹P NMR (162 MHz, CDCl₃): δ 18.3.

Synthesis of *trans*-Pt₂(PPh₂PhNMe₂)₂ (5)

Compound **4** (49.8 mg, 0.057 mmol) and CH₃I (40.0 μL, 92.0 mg, 0.65 mmol) were mixed in 20.0 mL CH₂Cl₂ and the mixture stirred at reflux for 2 days. The solvent was then evaporated under vacuum to give the crude product, which was purified by column chromatography using CH₂Cl₂/petroleum ether (5:4; v/v) as the eluent. Yield: 37.3 mg (63% based on Pt). Yellow single crystals of **5** were obtained by slow evaporation of a CH₂Cl₂/MeOH solution of **5** at r.t. Elemental analysis (%) for C₄₀H₄₀I₂N₂P₂Pt: Calcd C 45.34, H 3.81, N 2.64; found: C 44.84, H 3.68, N 2.6. IR (KBr disc, cm⁻¹): 3076 (vw), 2895(vw), 1594(vs), 1518(m), 1445(m), 1435(m), 1373(vs), 1293 (m), 1236(w), 1181(s), 1102(s), 1000(m), 949(w), 811(s), 745(s), 695(s), 624(s). NMR was not available due to the poor solubility of this compound.

Preparation of the nanoparticle of 1

Compound **1** (6.9 mg, 8.7 μmol) was dissolved in 2 mL DMSO at 60 °C, and then 1 mL of DMSO solution containing Pluronic® F-127 (20.1 mg, 1.6 μmol) was added. Dichloromethane (2.0 mL) was added to assist the dissolution and the mixture was stirred overnight at 60 °C to evaporate the CH₂Cl₂. The resulting solution was added to stirring water at a rate of 60 μL per minute (rotating speed 1400 rpm). After stirring for an additional 6 hours, the mixture was dialyzed (molecular weight cut-off: 3500) for 12 hours to obtain 15.0 mL of micellar solution. ³¹P NMR (162 MHz, CDCl₃): δ 14.3. The Pt concentration was determined to be 1.9 μg mL⁻¹ by ICP-MS. The solution was lyophilized for the *in vitro* experiments.

Preparation of nanoparticles of 2

Compound **2** (6.9 mg, 4.6 μmol) and Pluronic® F-127 (21.1 mg, 1.7 μmol) were mixed in CH₂Cl₂ (2.0 mL). After stirring for 10 hours, this mixture was added to 8.0 mL H₂O (rotating speed 1400 rpm) at a rate of 30 μL per minute. After stirring for 12 hours, the CH₂Cl₂ had evaporated, and the mixture was dialyzed (molecular weight cut-off: 3500) for 12 hours to obtain 8.0 mL of micellar solution. ³¹P NMR (162 MHz, CDCl₃): δ 14.3, 21.4. The Pt concentration was determined to be 41.3 μg mL⁻¹ by ICP-MS. The solution was lyophilized for *in vitro* experiments.

Preparation of nanoparticle of 3

Compound **3** (3.9 mg, 4.6 μmol) was dissolved in 1 mL of CH₂Cl₂, and 2.0 mL of DMSO containing Pluronic® F-127 (20.1 mg, 1.6 μmol). The mixture was stirred at 60 °C overnight to evaporate the CH₂Cl₂, and the resulting DMSO solution was added to stirring water (3.0 mL) at a rate of 30 μL per minute (rotating speed 1400 rpm). The mixture was stirred for a further 6 hours and then dialyzed (molecular weight cut-off: 3500) for 12 hours to obtain 8.0 mL micelle solution. ³¹P NMR (162 MHz, CDCl₃): δ 18.4, 10.7. The Pt concentration was determined to be 8.3 μg mL⁻¹ by ICP-MS. The solution was lyophilized for the *in vitro* experiments.

Preparation of the nanoparticle of 4

Compound **4** (5.3 mg, 6.0 μmol) was dissolved in a mixture of DMSO (4.0 mL) and CH₂Cl₂ (2.0 mL) and heated at 60 °C. A DMSO (1.0 mL) solution containing Pluronic® F-127 (20.0 mg, 1.6 μmol) was then introduced with stirring. The resulting mixture was stirred at 60 °C overnight to evaporate the CH₂Cl₂, and then added to stirring water at a speed of 30 μL per minute (1400 rpm). After stirring for an additional 6 hours, the mixture was dialyzed (molecular weight cut-off: 3500) for 24 hours to obtain 18.0 mL

micellar solution. ³¹P NMR (162 MHz, CDCl₃): δ 12.3. The Pt concentration was determined to be 8.4 μg mL⁻¹ by ICP-MS. The solution was lyophilized for the *in vitro* experiments.

X-ray crystallographic determination of 1–5

Single crystals of **1–5** were analyzed on a Bruker APEX III CCD X-ray diffractometer with graphite monochromated Ga Kα (λ = 1.34138 Å for **1**) and Mo Kα (λ = 0.71073 Å for **2–5**) radiations. Refinements and reductions of the collected data were achieved using the Bruker SAINT program and applied to all complexes with absorption correction (*multi-scan*).^[44] All crystal structures were solved by direct methods and refined on F² by full-matrix least-squares techniques with the SHELXTL-2016 program.^[3]

In complex **2**, a large amount of spatially delocalized electron density in the lattice was found but acceptable refinement could not be obtained for this electron density. The solvent contribution was then modeled using SQUEEZE in the Platon program suite.^[45] In complex **3**, the hydrogen atoms on the H₂O solvate were located from the difference Fourier map with their O–H distances fixed to O–H = 0.83 Å and thermal parameters constrained to U_{iso}(H) = 1.2 U_{eq}(O). The H₂O molecule was then refined as a rigid group. The hydrogen atoms on the N atom were added by using HFIX 23.

Crystallographic data for **1–5** have been deposited in the Cambridge Crystallographic Data Center (CCDC) as supplementary publication numbers 2092988–2092992. These data can be obtained free of charge either from the CCDC via www.ccdc.cam.ac.uk/data_request/cif or from the Supporting Information. A summary of the key crystallographic data for **1–5** are listed in Table 1.

Cytotoxicity evaluation by MTT assay

The B16F10 cell line was purchased from the Shanghai Institute of Cell Biology, Chinese Academy of Sciences. Fetal bovine serum (FBS), penicillin, streptomycin, and trypsin were purchased from Zhejiang Tianhang Biotechnology Co. Ltd. and used as supplied. The B16F10 cell lines were cultured in DMEM containing 10% FBS and 1% penicillin/streptomycin (P/S). Cells grew as a monolayer and were detached upon confluence using trypsin (0.5% w/v in PBS). The cells were harvested from the cell culture medium by incubating in trypsin solution for 3 min. The cells were centrifuged, and the supernatant discarded. A 3 mL portion of serum-supplemented cell culture medium was added to neutralize any residual trypsin. The cells were re-suspended in serum-supplemented DMEM at a concentration of 5 × 10⁴ cells per 1 mL. Cells were cultured at 37 °C and 5% CO₂ for the MTT studies.

B16F10 cells were seeded at a density of 1 × 10⁴ cells per well in 200 μL of DMEM (10% FBS + 1% P/S), and cultured for 16 h for attachment. The culture medium was then replaced by a serum-free medium containing various concentrations of the nanoformulations of **1–4**. After incubation with a period of 20 h, the MTT solution (100 μL, 0.5 mg mL⁻¹ in serum-free DMEM) was added to replace the cell culture medium. After incubating the cells at 37 °C for 4 h, the MTT solution was removed and DMSO (100 μL) added to dissolve the formazan crystals formed, and the microplates were agitated for 5 min at a medium rate before spectrophotometric measurement at 570 nm on a microplate reader. The untreated cells served as the 100% cell viability control, while the completely dead cells served as the blank. All experiments were carried out with five replicates (n = 5). The relative cell viability (%) related to control cells was calculated by the formula below:

$$V\% = \frac{[A]_{\text{experimental}} - [A]_{\text{blank}}}{[A]_{\text{control}} - [A]_{\text{blank}}} \times 100\%$$

wherein $V\%$ is the percentage of cell viability, $[A]_{\text{experimental}}$ is the absorbance of the wells culturing the treated cells, $[A]_{\text{blank}}$ is the absorbance of the blank, and $[A]_{\text{control}}$ is the absorbance of the wells culturing untreated cells.

Acknowledgments

This work was financially supported by the National Natural Science Foundation of China (Grant Nos. 21871203 and 51873185).

Conflict of Interest

The authors declare no conflict of interest.

Keywords: anticancer drug · Pt drugs · B16F10 · Pt–S cluster · crystal structure · *trans* effect

- [1] B. Rosenberg, L. Van Camp, T. Krigas, *Nature* **1965**, *205*, 698–699.
- [2] a) T. C. Johnstone, K. Suntharalingam, S. J. Lippard, *Chem. Rev.* **2016**, *116*, 3436–3486; b) J. J. Wilson, S. J. Lippard, *Chem. Rev.* **2014**, *114*, 4470–4495.
- [3] K. M. Deo, D. L. Ang, B. McGhie, A. Rajamanickam, A. Dhiman, A. Khoury, J. Holland, A. Bjelosevic, B. Pages, C. Gordon, J. R. Aldrich-Wright, *Coord. Chem. Rev.* **2018**, *375*, 148–163.
- [4] a) R. G. Kenny, C. J. Marmion, *Chem. Rev.* **2019**, *119*, 1058–1137; b) A. Annunziata, M. E. Cucciolo, R. Esposito, G. Ferraro, D. M. Monti, A. Merlino, F. Ruffo, *Eur. J. Inorg. Chem.* **2020**, *2020*, 918–929; c) J. X. Ong, H. V. Le, V. E. Y. Lee, W. H. Ang, *Angew. Chem. Int. Ed.* **2021**, *60*, 9264–9269; d) V. E. Y. Lee, Z. C. Lim, S. L. Chew, W. H. Ang, *Inorg. Chem.* **2021**, *60*, 1823–1831; e) M. J. R. Tham, M. V. Babak, W. H. Ang, *Angew. Chem. Int. Ed.* **2020**, *59*, 19070–19078; *Angew. Chem.* **2020**, *132*, 19232–19240; f) S. Jin, N. Muhammad, Y. Sun, Y. Tan, H. Yuan, D. Song, Z. Guo, X. Wang, *Angew. Chem. Int. Ed.* **2020**, *51*, 23313–23321; g) Q. Cao, D.-J. Zhou, Z.-Y. Pan, G.-G. Yang, H. Zhang, L.-N. Ji, Z.-W. Mao, *Angew. Chem. Int. Ed.* **2020**, *59*, 18556–18562; *Angew. Chem.* **2020**, *132*, 18715–18721; h) K. Wang, C. Zhu, Y. He, Z. Zhang, W. Zhou, N. Muhammad, Y. Guo, X. Wang, Z. Guo, *Angew. Chem. Int. Ed.* **2019**, *58*, 4638–4643; *Angew. Chem.* **2019**, *131*, 4686–4691; i) H. Shi, C. Imberti, P. J. Sadler, *Inorg. Chem. Front.* **2019**, *6*, 1623–1638; j) D. Hu, C. Yang, C.-N. Lok, F. Xing, P.-Y. Lee, Y. M. E. Fung, H. Jiang, C.-M. Che, *Angew. Chem. Int. Ed.* **2019**, *58*, 10914–10918; *Angew. Chem.* **2019**, *131*, 11030–11034; k) A. Eskandari, A. Kundu, S. Ghosh, K. Suntharalingam, *Angew. Chem. Int. Ed.* **2019**, *58*, 12059–12064; *Angew. Chem.* **2019**, *131*, 12187–12192.
- [5] a) M. Ghaferi, M. J. Asadollahzadeh, A. Akbarzadeh, H. Ebrahimi Shahmabadi, S. E. Alavi, *Int. J. Mol. Sci.* **2020**, *21*, 559; b) S.-X. Lin, W.-L. Pan, R.-J. Niu, Y. Liu, J.-X. Chen, W.-H. Zhang, J.-P. Lang, D. J. Young, *Dalton Trans.* **2019**, *48*, 5308–5314; c) N. Wang, Z. Wang, Z. Xu, X. Chen, G. Zhu, *Angew. Chem. Int. Ed.* **2018**, *57*, 3426–3430; *Angew. Chem.* **2018**, *130*, 3484–3488; d) Y. Li, Z. Gao, F. Chen, C. You, H. Wu, K. Sun, P. An, K. Cheng, C. Sun, X. Zhu, B. Sun, *ACS Appl. Mater. Interfaces* **2018**, *10*, 30930–30935; e) R. Zhang, X. Song, C. Liang, X. Yi, G. Song, Y. Chao, Y. Yang, K. Yang, L. Feng, Z. Liu, *Biomaterials* **2017**, *138*, 13–21.
- [6] a) N. Seetharamu, E. Kim, H. Hochster, F. Martin, F. Muggia, *Anticancer Res.* **2010**, *30*, 541–545; b) D. M. Vail, I. D. Kurzman, P. C. Glawe, M. G. O'Brien, R. Chun, L. D. Garrett, J. E. Obradovich, R. M. Fred, C. Khanna, G. T. Colbern, P. K. Working, *Cancer Chemother. Pharmacol.* **2002**, *50*, 131–136.
- [7] a) G. P. Stathopoulos, J. Stathopoulos, J. Dimitroulis, *Oncol Lett* **2012**, *4*, 1013–1016; b) T. Boulikas, *Expert Opin. Invest. Drugs* **2009**, *18*, 1197–1218.
- [8] a) D. Liu, C. He, A. Z. Wang, W. Lin, *Int. J. Nanomed.* **2013**, *8*, 3309–3319; b) M. J. A. de Jonge, M. Slingerland, W. J. Loos, E. A. C. Wiemer, H. Burger, R. H. J. Mathijssen, J. R. Kroep, M. A. G. den Hollander, D. van der Biessen, M.-H. Lam, J. Verweij, H. Gelderblom, *Eur. J. Cancer* **2010**, *46*, 3016–3021.
- [9] F. Zahednezhad, P. Zakeri-Milani, J. Shahbazi Mojarrad, H. Valizadeh, *Expert Opin. Drug Delivery* **2020**, *17*, 523–541.
- [10] a) H. Maeda, J. Wu, T. Sawa, Y. Matsumura, K. Hori, *J. Control. Release* **2000**, *65*, 271–284; b) J. W. Nichols, Y. H. Bae, *J. Control. Release* **2014**, *190*, 451–464.
- [11] a) P. a Ma, H. Xiao, C. Yu, J. Liu, Z. Cheng, H. Song, X. Zhang, C. Li, J. Wang, Z. Gu, J. Lin, *Nano Lett.* **2017**, *17*, 928–937; b) J. R. Pereira, S. J. Martins, S. M. Nikaedo, F. K. Ikari, *BMC Cancer* **2004**, *4*, 69; c) J. Guo, Z. Yu, M. Das, L. Huang, *ACS Nano* **2020**, *14*, 5075–5089.
- [12] S. Dhar, Z. Liu, J. Thomale, H. Dai, S. J. Lippard, *J. Am. Chem. Soc.* **2008**, *130*, 11467–11476.
- [13] a) Y. Zhai, W. Ran, J. Su, T. Lang, J. Meng, G. Wang, P. Zhang, Y. Li, *Adv. Mater.* **2018**, *30*, 1802378; b) C. He, C. Poon, C. Chan, S. D. Yamada, W. Lin, *J. Am. Chem. Soc.* **2016**, *138*, 6010–6019; c) L. M. de Freitas, C. P. Soares, C. R. Fontana, *J. Photochem. Photobiol. B* **2014**, *140*, 365–373; d) W. Zhang, J. Shen, H. Su, G. Mu, J. H. Sun, C. P. Tan, X. J. Liang, L. N. Ji, Z. W. Mao, *ACS Appl. Mater. Interfaces* **2016**, *8*, 13332–13340; e) P. Kroon, E. Frijlink, V. Iglesias-Guimaraes, A. Volkov, M. M. van Buuren, T. N. Schumacher, M. Verheij, J. Borst, I. Verbrugge, *Cancer Immunol. Res.* **2019**, *7*, 670–682; f) M. Hanif, C. G. Hartinger, *Future Med. Chem.* **2018**, *10*, 615–617; g) P. R. Brock, R. Maibach, M. Childs, K. Rajput, D. Roebuck, M. J. Sullivan, V. Lathier, M. Ronghe, P. Dall'Igna, E. Hiyama, B. Brichard, J. Skeen, M. E. Mateos, M. Capra, A. A. Rangaswami, M. Ansari, C. Rechnitzer, G. J. Veal, A. Covezzoli, L. Brugières, G. Perilongo, P. Czauderna, B. Morland, E. A. Neuwelt, *N. Engl. J. Med.* **2018**, *378*, 2376–2385.
- [14] a) N. Nagai, T. Isaka, S. Deguchi, M. Minami, M. Yamaguchi, H. Otake, N. Okamoto, Y. Nakazawa, *Int. J. Mol. Sci.* **2020**, *21*, 7083; b) M. Wu, W. Wu, Y. Duan, X. Liu, M. Wang, C. U. Phan, G. Qi, G. Tang, B. Liu, *Adv. Mater.* **2020**, 2005222.
- [15] H.-K. Fun, S. Chantrapromma, Y.-C. Liu, Z.-F. Chen, H. Liang, *Acta Crystallogr. Sect. E* **2006**, *62*, m1252–m1254.
- [16] H. A. Brune, M. Falck, R. Hemmer, G. Schmidtberg, H. G. Alt, *Chem. Ber.* **1984**, *117*, 2791–2802.
- [17] a) S. H. Chong, L. L. Koh, W. Henderson, T. S. A. Hor, *Chem. Asian J.* **2006**, *1*, 264–272; b) S. W. Audi Fong, T. S. Andy Hor, *J. Chem. Soc. Dalton Trans.* **1999**, 639–652; c) M. Zhou, Y. Xu, C.-F. Lam, P.-H. Leung, L.-L. Koh, K. F. Mok, T. S. A. Hor, *Inorg. Chem.* **1994**, *33*, 1572–1574.
- [18] a) M. Yu, J. Zheng, *ACS Nano* **2015**, *9*, 6655–6674; b) J. Liu, M. Yu, C. Zhou, S. Yang, X. Ning, J. Zheng, *J. Am. Chem. Soc.* **2013**, *135*, 4978–4981.
- [19] a) J. Zhou, L. Rao, G. Yu, T. R. Cook, X. Chen, F. Huang, *Chem. Soc. Rev.* **2021**, *50*, 2839–2891; b) H. Chen, W. Zhang, G. Zhu, J. Xie, X. Chen, *Nat. Rev. Mater.* **2017**, *2*, 17024; c) C. Lazzari, *Ther. Adv. Med. Oncol.* **2018**, *10*, 1–12; d) K. Ni, G. Lan, Y. Song, Z. M. Hao, W. Lin, *Chem. Sci.* **2020**, *11*, 7641–7653; e) S. F. Ngiow, G. A. McArthur, M. J. Smyth, *Cancer Cell* **2015**, *27*, 434–438.
- [20] A. I. Solomatina, A. D. Slobodina, E. V. Ryabova, O. I. Bolshakova, P. S. Chelushkin, S. V. Sarantseva, S. P. Tunik, *Bioconjug. Chem.* **2020**, *31*, 2628–2637.
- [21] S. Rottenberg, C. Disler, P. Perego, *Nat. Rev. Cancer* **2021**, *21*, 37–50.
- [22] a) F. Shen, L. Feng, Y. Zhu, D. Tao, J. Xu, R. Peng, Z. Liu, *Biomaterials* **2020**, *255*, 120190; b) A. Tesniere, F. Schlemmer, V. Boige, O. Kepp, I. Martins, F. Ghiringhelli, L. Aymeric, M. Michaud, L. Apetoh, L. Barault, J. Mendiboune, J. P. Pignon, V. Jooste, P. van Endert, M. Ducreux, L. Zitvogel, F. Piard, G. Kroemer, *Oncogene* **2010**, *29*, 482–491; c) P. Perego, J. Robert, *Cancer Chemother. Pharmacol.* **2016**, *77*, 5–18.
- [23] a) L. Zhou, P. Zhang, H. Wang, D. Wang, Y. Li, *Acc. Chem. Res.* **2020**, *53*, 1761–1772; b) X. Duan, C. Chan, W. Lin, *Angew. Chem. Int. Ed.* **2019**, *58*, 670–680; *Angew. Chem.* **2019**, *131*, 680–691; c) L. Wang, R. Guan, L. Xie, X. Liao, K. Xiong, T. W. Rees, Y. Chen, L. Ji, H. Chao, *Angew. Chem. Int. Ed.* **2021**, *60*, 4657–4665; *Angew. Chem.* **2021**, *133*, 4707–4715; d) J. Shen, T. W. Rees, L. Ji, H. Chao, *Coord. Chem. Rev.* **2021**, *443*, 214016.
- [24] D. Y. Q. Wong, W. W. F. Ong, W. H. Ang, *Angew. Chem. Int. Ed.* **2015**, *54*, 6483–6487; *Angew. Chem.* **2015**, *127*, 6583–6587.
- [25] R. C. Todd, S. J. Lippard, *Metallomics* **2009**, *1*, 280–291.
- [26] T. C. Johnstone, J. J. Wilson, S. J. Lippard, *Inorg. Chem.* **2013**, *52*, 12234–12249.

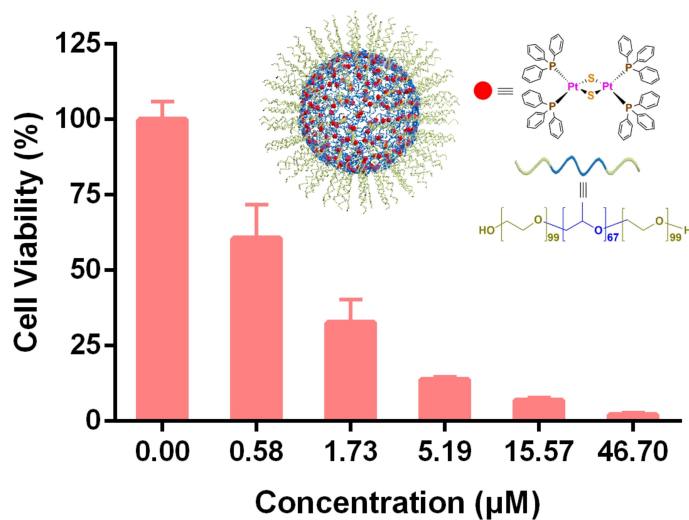
- [27] a) G. K. Anderson, H. C. Clark, J. A. Davies, G. Ferguson, M. Parvez, *J. Crystallogr. Spectrosc. Res.* **1982**, *12*, 449–458; b) R. Ugo, G. La Monica, S. Cenini, A. Segre, F. Conti, *J. Chem. Soc. A* **1971**, 522–528.
- [28] a) L. Pan, Q. He, J. Liu, Y. Chen, M. Ma, L. Zhang, J. Shi, *J. Am. Chem. Soc.* **2012**, *134*, 5722–5725; b) Q.-L. Zhang, D. Zheng, X. Dong, P. Pan, S.-M. Zeng, F. Gao, S.-X. Cheng, X.-Z. Zhang, *J. Am. Chem. Soc.* **2021**, *143*, 5127–5140; c) L. Zhang, D. Jing, N. Jiang, T. Rojalin, C. M. Baehr, D. Zhang, W. Xiao, Y. Wu, Z. Cong, J. J. Li, Y. Li, L. Wang, K. S. Lam, *Nat. Nanotechnol.* **2020**, *15*, 145–153; d) L. Zhang, Y. Huang, A. R. Lindstrom, T.-Y. Lin, K. S. Lam, Y. Li, *Theranostics* **2019**, *9*, 7807–7825.
- [29] X. Ling, D. Gong, W. Shi, Z. Xu, W. Han, G. Lan, Y. Li, W. Qin, W. Lin, *J. Am. Chem. Soc.* **2021**, *143*, 1284–1289.
- [30] a) J. X. Chen, W. H. Zhang, X. Y. Tang, Z. G. Ren, H. X. Li, Y. Zhang, J. P. Lang, *Inorg. Chem.* **2006**, *45*, 7671–7680; b) J. X. Chen, W. H. Zhang, X. Y. Tang, Z. G. Ren, Y. Zhang, J. P. Lang, *Inorg. Chem.* **2006**, *45*, 2568–2580.
- [31] H. Li, G. B. Carpenter, D. A. Sweigart, *Organometallics* **2000**, *19*, 1823–1825.
- [32] a) Y. Liu, S.-X. Lin, R.-J. Niu, Q. Liu, W.-H. Zhang, D. J. Young, *ChemPlusChem* **2020**, *85*, 832–837; b) M. Armaghan, X. J. Shang, Y. Q. Yuan, D. J. Young, W. H. Zhang, T. S. A. Hor, J. P. Lang, *ChemPlusChem* **2015**, *80*, 1231–1234; c) M. Armaghan, W. Y. J. Lu, D. Wu, Y. Wei, F.-L. Yuan, S. W. Ng, M. M. Amini, W.-H. Zhang, D. J. Young, T. S. A. Hor, J.-P. Lang, *RSC Adv.* **2015**, *5*, 42978–42989.
- [33] a) T. Karasawa, P. S. Steyger, *Toxicol. Lett.* **2015**, *237*, 219–227; b) D. J. Crona, A. Faso, T. F. Nishijima, K. A. McGraw, M. D. Galsky, M. I. Milowsky, *Oncologist* **2017**, *22*, 609–619.
- [34] C. He, D. Liu, W. Lin, *ACS Nano* **2015**, *9*, 991–1003.
- [35] S. Jenni, G. Picci, M. Fornasier, M. Mamusa, J. Schmidt, Y. Talmon, A. Sour, V. Heitz, S. Murgia, C. Caltagirone, *Photochem. Photobiol. Sci.* **2020**, *19*, 674–680.
- [36] S. D. Adhikary, D. Bose, P. Mitra, K. D. Saha, V. Bertolasi, J. Dinda, *New J. Chem.* **2012**, *36*, 759–767.
- [37] A. L. d A Querino, K. B. Enes, O. A. Chaves, D. Dittz, M. R. C. Couri, R. Diniz, H. Silva, *Bioorg. Chem.* **2020**, *100*, 103936.
- [38] E. E. Aranda, T. A. Matias, K. Araki, A. P. Vieira, E. A. de Mattos, P. Colepicolo, C. P. Luz, F. L. N. Marques, A. M. da Costa Ferreira, *J. Inorg. Biochem.* **2016**, *165*, 108–118.
- [39] G. Horvath, T. Premkumar, A. Boztas, E. Lee, S. Jon, K. E. Geckeler, *Mol. Pharm.* **2008**, *5*, 358–363.
- [40] S. S. Shrikhande, D. S. Jain, R. B. Athawale, A. N. Bajaj, P. Goel, Z. Kamran, Y. Nikam, R. Gude, *Saudi Pharm. J.* **2015**, *23*, 341–351.
- [41] M. H. Johansson, S. Otto, *Acta Crystallogr. Sect. C* **2000**, *56*, e12–e15.
- [42] a) M. Zhou, Y. Xu, A.-M. Tan, P.-H. Leung, K. F. Mok, L. L. Koh, T. S. A. Hor, *Inorg. Chem.* **1995**, *34*, 6425–6429; b) S. H. Chong, W. Henderson, T. S. A. Hor, *Dalton Trans.* **2007**, 4008–4016; c) J. Li, T. S. A. Hor, *Dalton Trans.* **2008**, 5708–5711.
- [43] a) K. D. Tew, *Cancer Res.* **2016**, *76*, 4313–4320; b) A. De Luca, L. J. Parker, W. H. Ang, C. Rodolfo, V. Gabbarini, N. C. Hancock, F. Palone, A. P. Mazzetti, L. Menin, C. J. Morton, M. W. Parker, M. Lo Bello, P. J. Dyson, *Proc. Natl. Acad. Sci. USA* **2019**, *116*, 13943–13951.
- [44] G. Sheldrick, *Acta Crystallogr. Sect. C* **2015**, *71*, 3–8.
- [45] A. L. Spek, *Acta Crystallogr. Sect. C* **2015**, *71*, 9–18.

Manuscript received: August 4, 2021

Accepted manuscript online: August 12, 2021

Version of record online: ■■■, ■■■■

FULL PAPER



P. Wang, Dr. J.-W. Wang, Prof. W.-H. Zhang*, Dr. H. Bai*, Prof. G. Tang, Prof. D. J. Young

1 – 9

In Vitro Anticancer Activity of Nanoformulated Mono- and Dinuclear Pt Compounds



Nanoformulations of a class of mononuclear and dinuclear Pt-based complexes bearing Pt–P bonds have

been developed as efficient chemotherapeutic reagents against murine melanoma cell line B16F10.